J Mater Sci (2009) 44:2581–2589
DOI 10.1007/s10853-009-3337-7

Influence of starch content and sintering temperature on the microstructure of porous yttria-stabilized zirconia tapes

María P. Albano · Liliana B. Garrido · Kevin Plucknett · Luis A. Genova

Received: 15 October 2008 / Accepted: 10 February 2009 / Published online: 6 March 2009

Abstract Porous yttria-stabilized zirconia (YSZ) substrates with volume fractions of porosity ranging from 28.9 to 53 vol.% were developed using starch as a fugitive additive. Concentrated aqueous YSZ slips with different amounts of starch and an acrylic latex binder were prepared. The influence of the volume fraction of starch and sintering temperature on the sintering behavior and final microstructure were investigated. Two kinds of pores were observed in the sintered tapes: large pores created by the starch particles with lengths between 15 and 80 μm and smaller pores in the matrix with lengths between 0.6 and 3.8 μm. The porosities were above those predicted for each of the starch contents. However, larger deviations from the predicted porosity were found as more starch was added. The top surface of the sintered tapes had a greater porosity than the bottom one for all the starch contents examined. The total porosity and the percentage of open porosity in the sintered tapes could be controlled by the volume fraction of added starch as well as by the sintering temperature. The open pores between the YSZ particles were removed by sintering at 1600 °C. As the volume fraction of starch increased from 17.6 to 37.8 vol.%, there was a gradual increase in the interconnectivity of the pore structure.

M. P. Albano (✉) · L. B. Garrido
Centro de Tecnología de Recursos Minerales y Cerámica (CETMIC), C.C. 49 (B1897ZCA), M. B. Gonnet, Provincia de Buenos Aires, Argentina
e-mail: palbano@cetmic.unlp.edu.ar

K. Plucknett
Department of Process Engineering and Applied Science, Dalhousie University, 1360 Barrington Street, Halifax, NS B3J 1Z1, Canada

L. A. Genova
Instituto de Pesquisas Energéticas e Nucleares (IPEN), Av. Lineu Prestes 2242-Cidade Universitária, CEP 05508-000 São Paulo, Brazil

Introduction

Porous ceramics have a number of important applications in devices that include filters, gas burners, bioceramics, fuel-cell electrodes, and membrane reactors, etc. [1–3]. In particular, Cu/YSZ and Ni/YSZ (cermet) tapes are used for anodes in solid oxide fuel cells (SOFC) [4–6]. As the cermet anode should be 30 vol.% metal to ensure electronic conductivity, and should still remain highly porous to allow diffusion of fuel to the electrolyte interface, very high initial porosity (~40 vol.%) is desirable for the YSZ substrate. Open porosity is required for the electrode to supply fuel and for removal of reaction products [5].

Many different manufacturing techniques are used to produce the ceramic layer. In this study, a porous YSZ matrix was developed by tape casting. One method to produce porous YSZ tapes is tape casting of YSZ with pore-forming agents. A carbon-based pyrolyzable pore former is mixed with the YSZ powder in the slurry preparation stage. The pore former is eliminated by combustion during the calcination at high temperature, leaving stable voids that are not removed during the subsequent sintering procedure [7, 8]. A material is obtained after sintering with porosity corresponding to the original amount, shape, and size of the starch particles. This method of introducing porosity offers a direct control over the porous characteristics of the final ceramic. In addition, it may be possible to form open pore networks because of the potential percolation of these pyrolyzable particles in the green body [7, 8]. Starch is one of the more frequently used pore-forming agents, because of its chemical composition and is easily

burnt out during firing without residues in the final ceramic body [9]. It has also been shown that the morphology and the size of the pores are particular to the type of starch used to create the porosity [10].

The tape-casting process for porous ceramics involves the preparation of a concentrated YSZ suspension with the addition of a pore-forming agent, a binder, and a plasticizer [11]. Aqueous-based tape casting offers several advantages due to the low-cost, non-toxic nature of the fluid vehicle. The development of such formulations has been a subject of recent research [12–14]. Kristoffersen et al. [13] evaluated different types of organic binders for aqueous tape casting of alumina. They found that latex binders yielded the highest solids loading suspensions, while still maintaining the appropriate rheological behavior. These emulsions have useful and unique characteristics such as internal plasticization and controllable crosslinking [14]. In the present study, we have developed an aqueous-based starch/YSZ/latex system for tape casting of porous ceramics.

The possibility of being able to control the microstructure of the porous YSZ tapes in terms of volume fraction of porosity, size, and geometry of the pores is crucial in order to target particular properties for the final ceramic. Therefore, in this study, the influence of the volume fraction of starch and sintering temperature on the sintering behavior and final microstructure were investigated. Details of the microstructure were observed by SEM.

Experimental procedure

Materials

A commercial yttria-doped YSZ powder (Y8Z01, Saint-Gobain, France) was used in this study. The mean particle diameter and the specific surface area were 0.53 μm and 8.26 m^2/g, respectively. Potato starch commercially available in Argentina was used as pore former agent. The starch granules exhibit a small degree of anisotropy with a median equivalent diameter of about 50 μm.

A commercial ammonium polyacrylate (NH_4PA) solution (Duramax D 3500, Rohm & Haas, Philadelphia, PA) was used as a dispersant. The binder was an acrylic latex emulsion (Duramax B1000, Rohm & Haas, Philadelphia, PA) with solid loading of 55 wt%, an average particle size of 0.37 μm, and a glass-transition temperature of −26 °C.

Slip preparation

Concentrated aqueous YSZ suspensions with a solid loading of 77 wt% were prepared by deagglomeration of the powder in distilled water with 0.3 wt.% NH_4PA (dry weight base of powder) using an ultrasonic bath. Different amounts of starch in the range of 13–33 wt% (dry weight base of YSZ powder) were added to the stabilized YSZ slips, followed by ultrasonic treatment. Subsequent to this, 25 wt.% latex (dry weight basis with respect to (YSZ + starch) powders) was added to the slurry, followed by additional stirring. The pH of the suspensions was adjusted to 9.0 with ammonia (25 wt.%).

Tape casting

The slips were cast manually on a Mylar film using an extensor. The gap between the extensor and the film was adjusted to 0.4 mm. The cast tapes were subsequently dried in air at room temperature up to constant weight; afterwards, they were stripped from the film.

Burnout and sintering

The burnout of organic additives was achieved by slow heating (1 °C/min) up to 1000 °C. Then, the pre-calcined tapes were sintered at 1300, 1400, 1500, and 1600 °C for 2 h, with a heating rate of 5 °C/min.

Characterization of green and sintered tapes

The tapes were weighted and measured geometrically to determine the green density. The bulk-sintered density was calculated from the dimensions and weight of the sintered pieces. In order to calculate the relative green and sintered densities, density values of 6.05 and 1.45 g/cm^3 were used for YSZ and starch, respectively.

The open porosity and the pore size distribution of the sintered tapes were determined using mercury porosimetry (Porosimeter 2000 Carlo Erba, Italy). The microstructure of green and sintered samples were observed on fractured surfaces using a field emission scanning electron microscopy (FE-SEM) (Hitachi S-4700).

Results and discussion

Table 1 shows the compositions of YSZ tapes with different amounts of starch. We can define the following expressions:

$$V_S = \text{volume of starch/bulk greenvolume}, (V_T) \quad (1)$$

$$V_S = \text{volume of starch/volume of starch} + \text{volume of YSZ} + \text{volume of latex} + \text{volume of pores}$$

$$F_{VS} = \text{volume of starch/volume of solids} \quad (2)$$

Table 1 Compositions of YSZ tapes with different amounts of starch

V_S (%)	F_{VS} (%)	F_{VZ} (%)	F_{VL} (%)	F_{VL}/F_{VZ}
0	0	42	58	1.38
17.6	19	31	50	1.61
28.4	30	25	45	1.82
37.8	40	19	41	2.16

$$F_{VS} = \text{volume of starch/volume of starch} + \text{volume of YSZ} + \text{volume of latex}$$

$$F_{VZ} = \text{volume of YSZ/volume of solids} \quad (3)$$

$$F_{VL} = \text{volume of latex/volume of solids} \quad (4)$$

V_S indicates the volume of starch relative to the volume of the green tape, whereas F_{VS} is the volume of starch with respect to the volume of solids.

The relative green density of the tapes with volume fraction of starch (V_S) between 0 and 37.8% was 93–95% of the theoretical density. The relative green density values were close to the theoretically predicted values. This indicates that some residual porosity, between 5 and 7% remained in the tapes. A certain amount of porosity can be generated by air trapped in the suspension or by incomplete mixing of the powders during processing [7]. In addition, drying can also create non-uniformly mixed powders in the green tape. Different settling behavior of the powder constituents and/or reagglomeration during solvent evaporation can also occur [7]. The volume fraction of starch in the green tape (V_S) was slightly lower than the volume fraction of added starch (F_{VS}), due to the presence of some residual porosity in the green body (Table 1).

The relative green density was kept nearly constant with increasing the amount of starch from 0 to 37.8%. This suggested that the addition of starch to the YSZ tape did not introduce additional porosity. Thus, as the starch content increased, the starch particle contact as a result of percolation did not contribute to a reduction in packing efficiency.

Figure 1 shows the bulk YSZ packing density (δ_{YSZ}) in the matrix as a function of F_{VL}/F_{VZ} ratio. The bulk YSZ packing density in the matrix can be expressed by:

$$\delta_{YSZ} = \text{volume of YSZ}/(V_T - \text{volume of starch}) \quad (5)$$

This parameter indicates the bulk packing density of the YSZ within the matrix, which is formed by the binder and pores, surrounding the starch particles.

As the amount of starch increased more latex was required to bind the particles, thereby increasing the F_{VL}/F_{VZ} ratio (Table 1). An approximately linear correlation between δ_{YSZ} and F_{VL}/F_{VZ} could be found; the added latex along with the starch decreased the bulk packing density of the YSZ powder within the matrix. This behavior has also been observed by our group in a previous study [15].

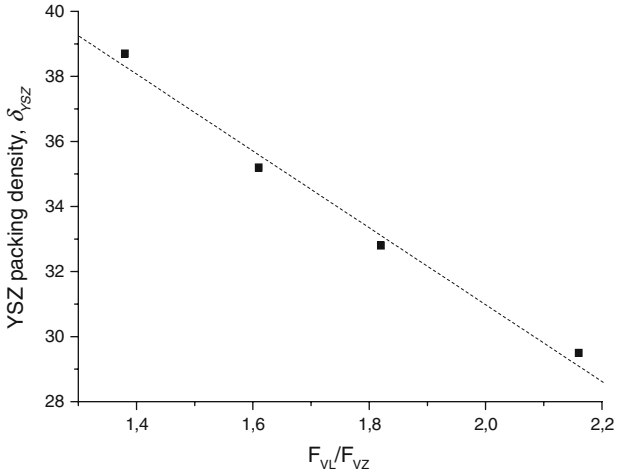

Fig. 1 Bulk YSZ packing density in the matrix as a function of F_{VL}/F_{VZ} ratio

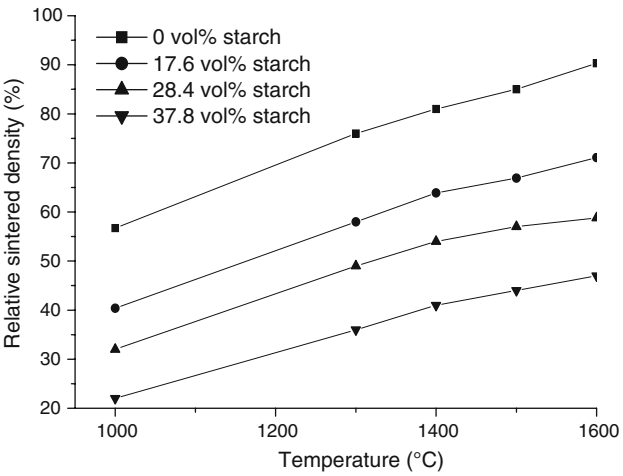

Fig. 2 Relative sintered density as a function of the sintering temperature for tapes with different volume fractions of starch

Figure 2 shows the relative sintered density as a function of the sintering temperature for tapes with different volume fraction of starch: 0, 17.6, 28.4, and 37.8%. The relative sintered density of the tapes increased with increasing the sintering temperature from 1000 to 1600 °C due to the densification of the YSZ matrix. At a given temperature, the relative sintered density of the tapes decreased as more starch was added.

Figure 3a and b shows the matrix of a tape without starch sintered at 1300 and 1600 °C, respectively. As the sintering temperature increased from 1300 to 1600 °C the following changes accompanied the densification: the formation of necks between YSZ grains-substituted grain boundaries areas for surface areas; the resulting network of porosity was reduced in volume, it coarsened and lost connectivity giving finally retained closed porosity on the grain boundaries. The relative sintered density of the tapes

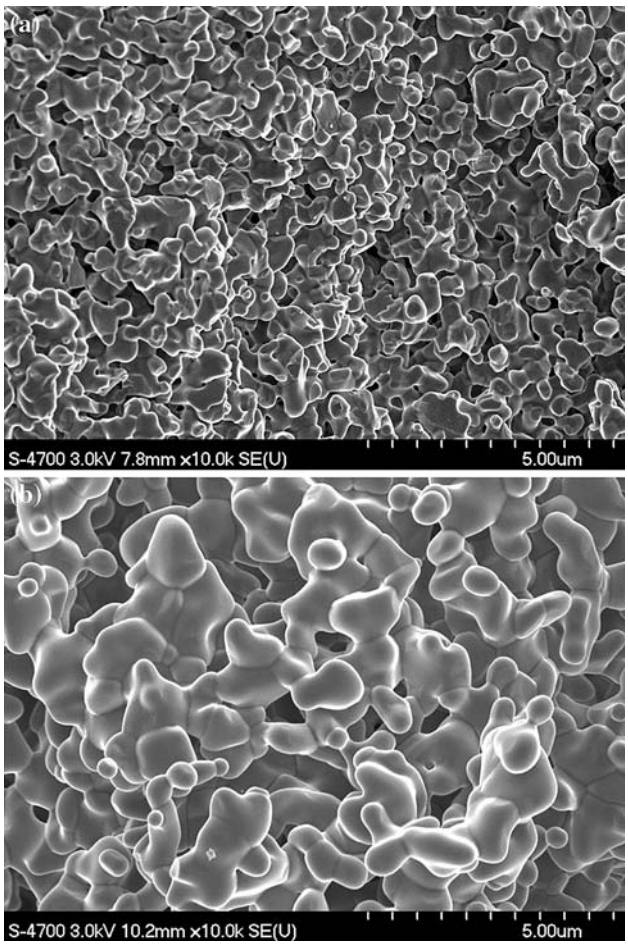

Fig. 3 The matrix microstructure of tapes without starch sintered at different temperatures: **a** 1300 °C, **b** 1600 °C

without starch sintered at 1600 °C was 90.3% of the theoretical density. Thus, the YSZ tapes did not achieve full densification at 1600 °C. This observation was also noted for the tapes prepared with starch sintered at 1600 °C. Figure 4 shows a SEM image of a tape with 17.6 vol.% starch sintered at 1600 °C. The microstructure consisted of large pores created by the starch particles with length between 15 and 80 μm and smaller pores in the matrix with length between 0.6 and 3.8 μm. Thus, some closed porosity remained in the YSZ matrix of the sintered tapes.

Figure 5 shows the total bulk porosity of the tapes sintered at 1600 °C versus the volume fraction of starch in the green tape; the 1:1 relationship between the bulk porosity and the amount of starch is shown. This relationship assumed that a full densification of the YSZ matrix occurred and consequently the remaining porosity corresponds to the volume fraction of starch originally added. Deviations from the 1:1 relationship could be seen, the porosities were above the predicted amount for all starch contents. Therefore, the higher porosity observed with respect to the amount of added starch was due to an

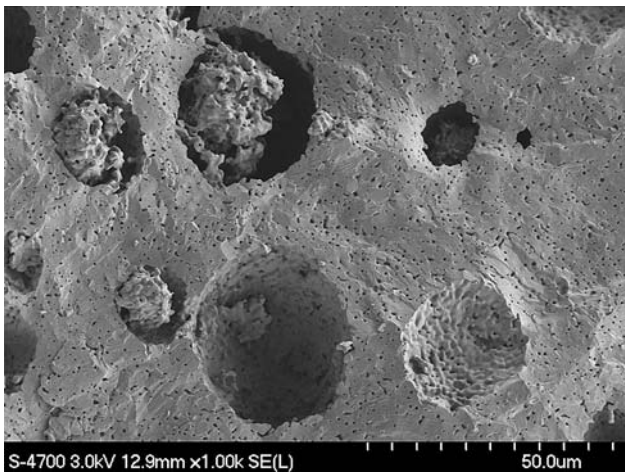

Fig. 4 SEM micrograph of a tape with 17.6 vol.% starch sintered at 1600 °C

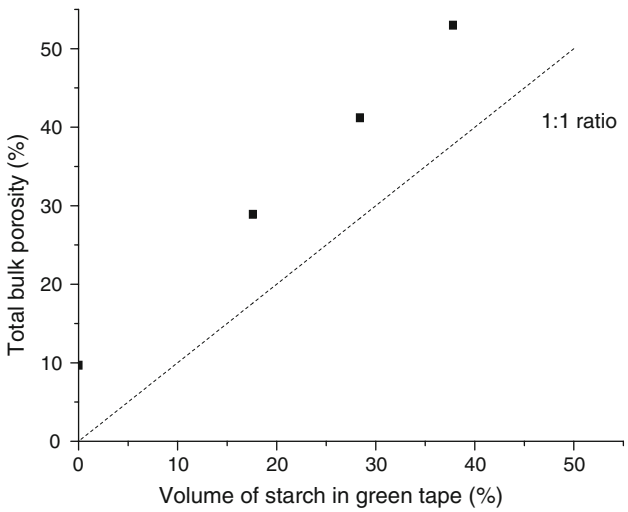

Fig. 5 Total bulk porosity of tapes sintered at 1600 °C versus the volume fraction of starch in the green tape

incomplete densification of the YSZ matrix during sintering (Figs. 2, 4).

Figure 6 shows the matrix of the tapes with 0 and 37.8 vol.% starch sintered at 1600 °C. The micrographs show rounded and elongated pores with length between 0.6 and 3.8 μm. The coalescence of the latex particles during drying and the pore coalescence during sintering might contribute to the enlargement of the pores in the matrix. The onset of the latex coalescence is expected to occur during the drying of the cast tapes when the volume fraction of latex particles approaches 0.6, its maximum solid loading [16]. The latex coalescence resulted in an increase in the particle size of the latex, thereby increasing the pore size left by the latex during burnout. The pores could also coalesce during sintering so that the pore size increased. The greater the pore size, the lower the driving force for

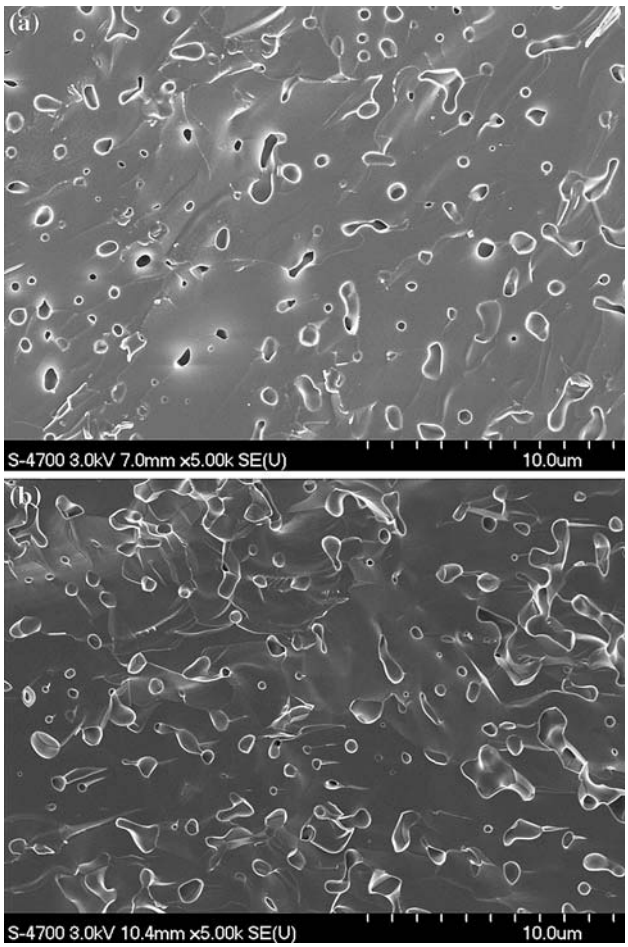

Fig. 6 The matrix microstructure of tapes sintered at 1600 °C with different volume fractions of starch: **a** 0, **b** 37.8%

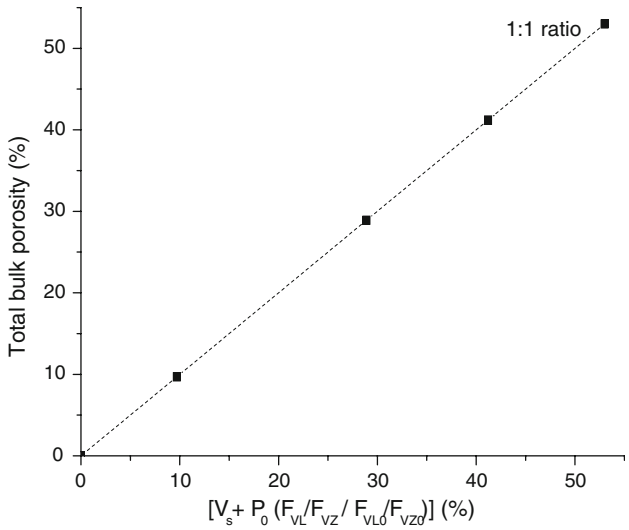

Fig. 7 Total bulk porosity of tapes sintered at 1600 °C versus $[V_S + P_0\ (F_{VL}/F_{VZ}/F_{VL0}/F_{VZ0})]$. V_S = volume fraction of starch in the green tape; P_0 = total porosity of the tapes without starch; $[F_{VL}/F_{VZ}/F_{VL0}/F_{VZ0}]$ = volume fraction of added latex/volume fraction of added YSZ, of the green tapes with starch relative to that of the tapes without starch

sintering and shrinkage [17]. The enlargement of the pores leads to a decreased sintering rate [17]. Therefore, the large pores in the matrix reduced the sinterability of the YSZ leading to retained closed porosity in the sintered tapes. As a consequence, the porosities were above those predicted for all the starch contents.

Larger deviations from the predicted porosity as more starch was added were observed in Fig. 5. An increase in the matrix porosity with increasing volume fraction of starch in the green tape was found in Fig. 6. The higher F_{VL}/F_{VZ} ratio for the tapes with increasing added starch decreased the YSZ packing density within the matrix, thereby increasing the matrix porosity after sintering at 1600 °C. Consequently, the larger deviations from the predicted porosity as more starch was added were attributed to the reduction in the YSZ packing density.

If the total bulk porosity of the tapes sintered at 1600 °C is plotted against $[V_S + P_0\ (F_{VL}/F_{VZ}/F_{VL0}/F_{VZ0})]$ (Fig. 7), the 1:1 relationship is followed. P_0 is the total porosity of the tapes without starch and the factor $[F_{VL}/F_{VZ}/F_{VL0}/F_{VZ0}]$ is the F_{VL}/F_{VZ} ratio of the green tapes with starch with respect to that of the tapes without starch. The term $[P_0\ (F_{VL}/F_{VZ}/F_{VL0}/F_{VZ0})]$ represents the additional porosity produced by the latex volume added with respect to the YSZ which increased as more starch was added. Clearly, the total porosity of the tapes followed that predicted based on the volume fraction of starch in the green tape and the additional porosity created by the adjustments of the formulation (higher F_{VL}/F_{VZ} ratio with increasing added starch).

Hg porosimetry was used to measure the smaller channels which corresponded to the connecting contacts voids between much larger pores created by the original starch particles. Figure 8a–d show the differential pore size distribution curves of tapes with 0, 17.6, 28.4, and 37.8 vol.% starch, sintered at different temperatures, respectively. An unimodal distribution of pore sizes was observed for the tapes with 0 and 17.6 vol.% starch sintered at 1000 and 1300 °C. The most frequent pore radius was 0.13–0.16 μm, which corresponded to the pores between the YSZ particles. The volume of pores between YSZ particles decreased with increasing the sintering temperature from 1000 to 1300 °C and disappeared at 1600 °C. The open porosity was completely removed at 1600 °C due to the development of necks between the YSZ grains.

For the tapes with 28.4 and 37.8 vol.% starch sintered at 1000 and 1300 °C, channels with sizes between 0.5 and 3 μm appeared, resulting in a bimodal distribution. These channels corresponded to the voids between the larger pores created by the starch particles. For 37.8 vol.% starch, the volume of the small pores between the YSZ particles was lower than the volume of the connecting channels, since the

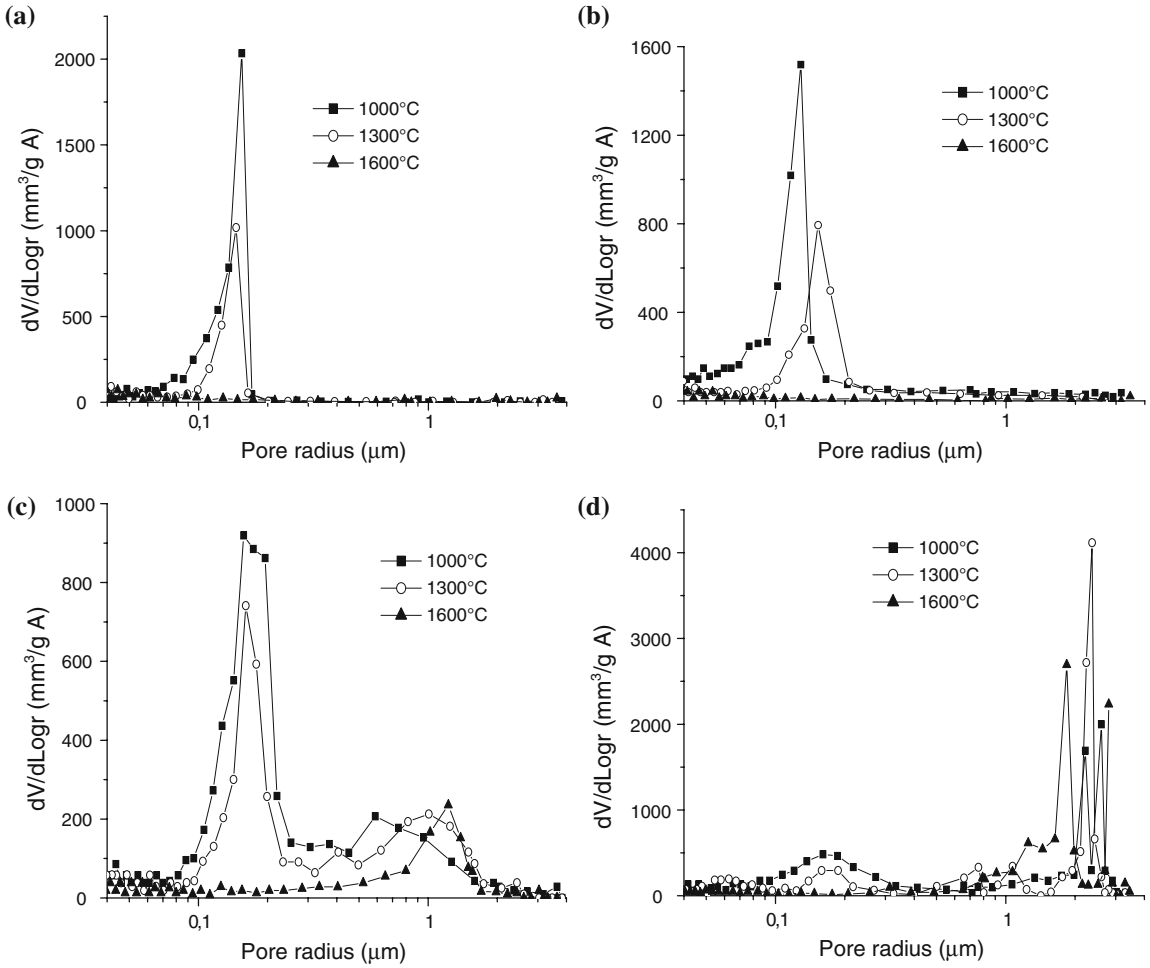

Fig. 8 Pore size distribution curves of tapes sintered at different temperatures with different volume fractions of starch: **a** 0%, **b** 17.6%, **c** 28.4%, **d** 37.8%

volume fraction of starch in the green tape was higher than the volume fraction of YSZ (Table 1). At 1600 °C, the pore size distribution changed from bimodal to unimodal due to the densification of the YSZ matrix; thus, the open porosity corresponded to the connecting channels between the overlapping starch pores which resulted in a connected porous network in the sintered body.

As more starch was added the number of contacts between the YSZ particles decreased, thereby decreasing the volume of pores between YSZ particles at temperatures lower than 1600 °C. As the volume fraction of starch increased from 28.4 to 37.8 vol.% at all the temperatures, the volume and size of the most frequent channels increased. The most frequent channel radius at 1600 °C was 1.29 μm for 28.4 vol.% starch and 1.82–2.75 μm for 37.8 vol.% starch. Thus, when the amount of starch increased the number of contacts between the starch particles also increased, resulting in more channels of larger sizes.

Figure 9 shows the open porosity percentage versus the sintering temperature for the different starch contents. The

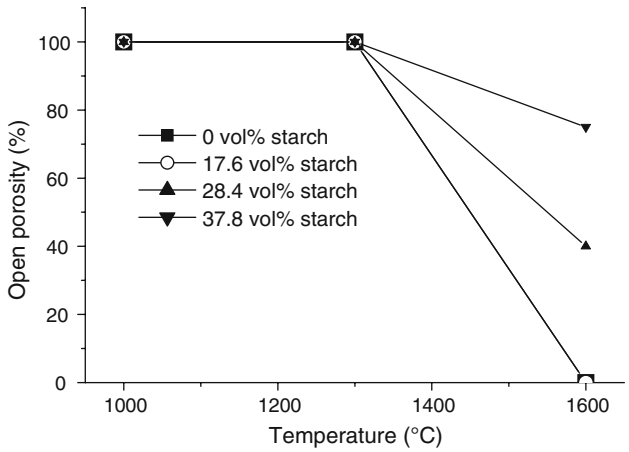

Fig. 9 Open porosity percentage versus sintering temperature for the different starch contents

porosity was completely open for the tapes with different amounts of starch sintered at 1000 and 1300 °C. This was expected since only limited densification of the YSZ matrix

had occurred at these temperatures. At 1600 °C, there was no measurable open porosity for amounts of starch ≤17.6 vol.%. There was a gradual increase in the openness of the pore structure with increasing the amount of added starch from 17.6 to 37.8 vol.%. This openness could be due to the gradual creation of percolating starch networks that extend through the green body and lead to connected porous networks in the sintered body. The percolation threshold of 17.6 vol.% corresponded well to the percolation threshold of approximately 18 vol.% found for porous alumina ceramics prepared with starch [18]. The level of interconnectivity between pores increased with increasing starch addition. Higher interconnectivity will open paths and channels between pores, which finally result in open porosity [19]. For 37.8 vol.% starch open porosity was predominant in the microstructure. The percentage of open porosity in the sintered tapes could be controlled by the volume fraction of starch added as well as by the sintering temperature.

Figure 10 shows a micrograph of a tape with 17.6 vol.% starch sintered at 1400 °C. Large elongated pores left by the starch and smaller pores between the YSZ grains could be seen. The wall surface microstructure of the large pores was observed and compared with that of the YSZ matrix, Figs. 11a and b, respectively. The matrix reached a higher densification than the interior surface of the pore. The higher densification of the matrix with respect to the pore wall surface, was evident by the following changes: the YSZ particles changed their shape by rounding off sharp corners, the necks between the YSZ grains growth, and the porosity at the grain boundaries was reduced in volume. A disruption in the packing of YSZ particles occurred in the first layer of particles around the starch granules in the green tape which became the pore wall in the sintered tape. As the YSZ particles of the first layer were not in contact with other particles, the diffusion mechanisms during sintering were less effective resulting in a lower densification.

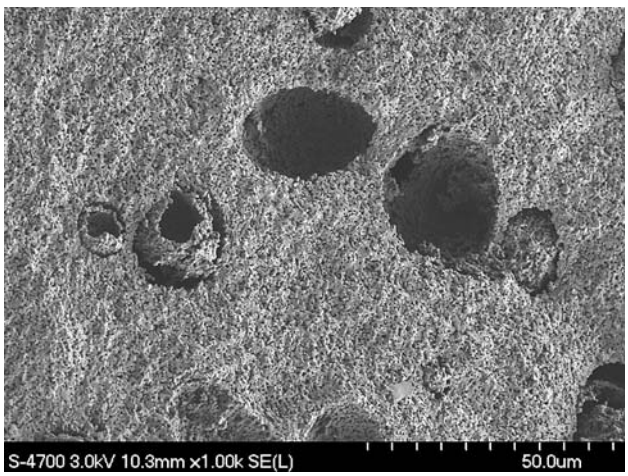

Fig. 10 SEM micrograph of a tape with 17.6 vol.% starch sintered at 1400 °C

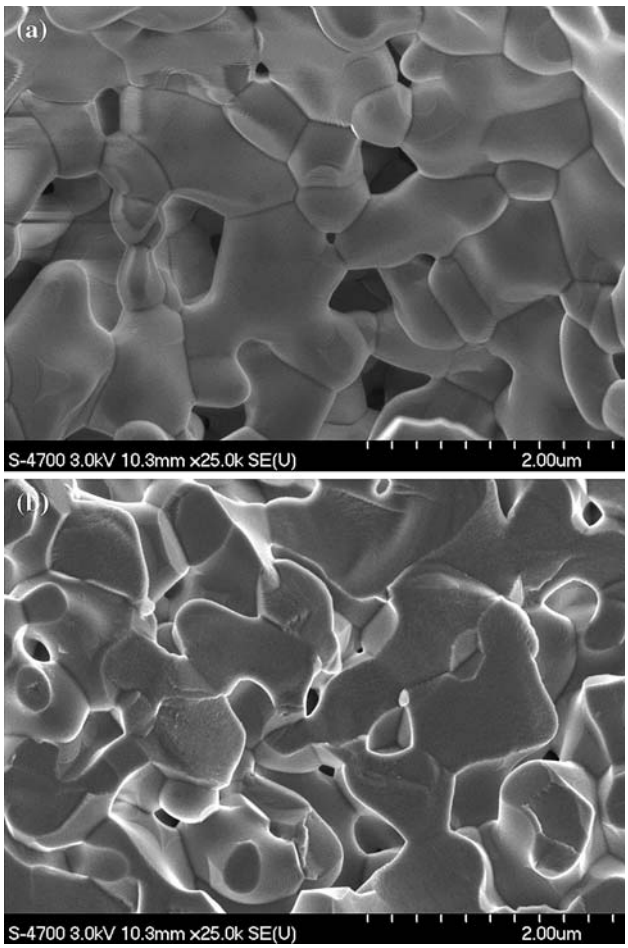

Fig. 11 **a** Wall surface microstructure of a large pore left by the starch, **b** Microstructure of the YSZ matrix

Some of the large pores left by the starch particles had inner shells of YSZ separated from the rest of the YSZ matrix (Fig. 10). These shells were previously observed using the starch processing method [18, 19]. There is some contraction of the starch particles during heating; a shell of ceramic particles, adhering to the surface of each starch particle, in the surrounding matrix is released from the rest of the matrix and follows the shrinking starch particles during heating [20]. Hence, a space between the formed shell of ceramic and the main ceramic matrix is left after sintering [20].

Figure 12 shows a SEM image of a large pore with the inner YSZ shell for a tape with 37.8 vol.% starch sintered at 1500 °C. A lower densification of the shell with respect to the matrix was also found. The lower densification was attributed to the separation of the shell YSZ particles from the rest of the matrix, thereby producing a disruption in the packing of YSZ particles.

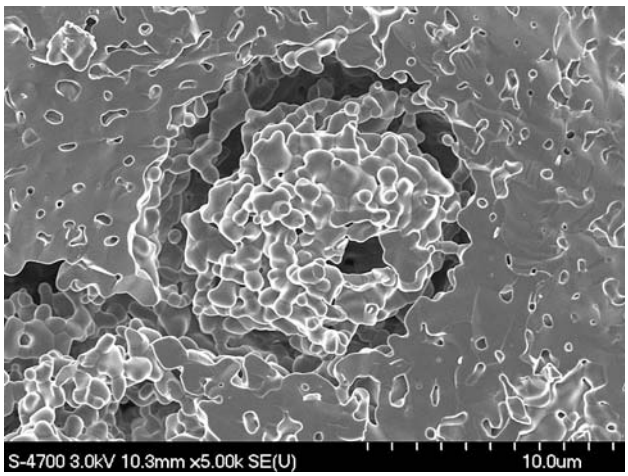

Fig. 12 SEM micrograph of a large pore with the inner YSZ shell for a tape with 37.8 vol.% starch sintered at 1500 °C

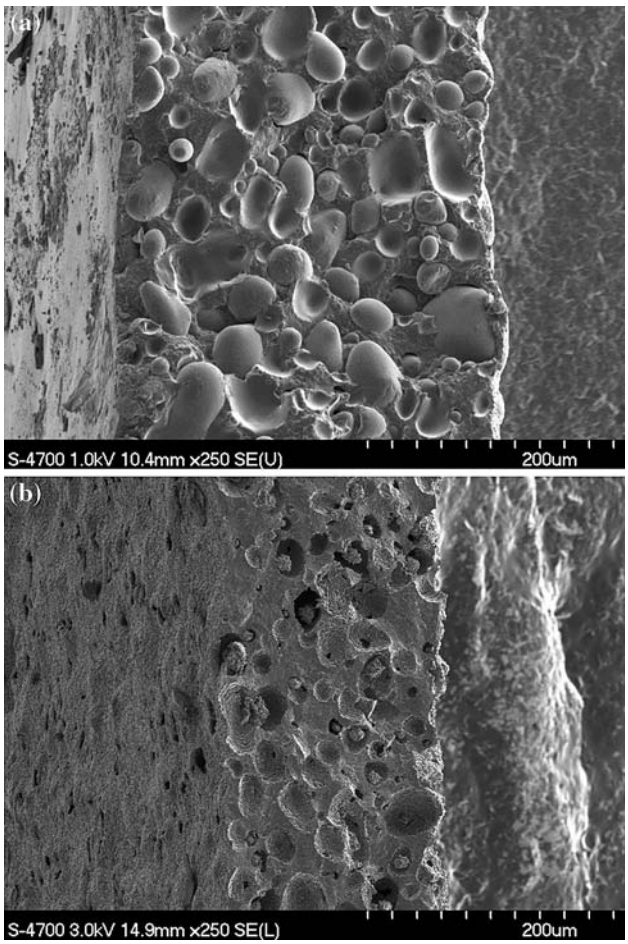

Fig. 13 SEM micrographs of **a** a green tape with 37.8 vol.% starch, **b** a tape with 37.8 vol.% starch sintered at 1600 °C

Figure 13a and b shows a green tape with 37.8 vol.% starch and the corresponding microstructure of the sintered tape at 1600 °C, respectively. It was evident that the shape and size of the pores corresponded well to the shape and size of the starch particles in the green body. Contraction of the tape was observed in the thickness direction. However, since the pores left by the starch were larger than the interstitial voids between the YSZ particles, they were not removed during sintering.

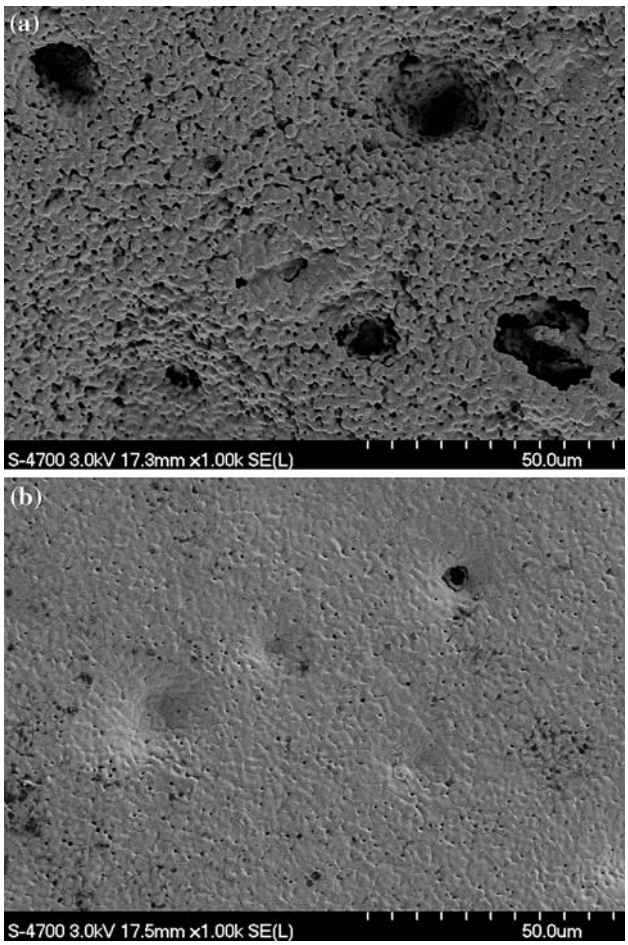

Fig. 14 SEM micrographs of different surfaces of a tape with 17.6 vol.% starch sintered at 1600 °C: **a** top surface, **b** bottom surface

Figure 14a and b shows micrographs of the top and bottom surfaces of a tape with 17.6 vol.% starch sintered at 1600 °C, respectively. The bottom surface was in contact with the film carrier during the drying process. As clearly shown, the surfaces were different: the top surface was rough whereas the bottom one was smooth, and the top surface had a greater porosity than the bottom one. This behavior was found for all the starch contents examined. During drying, the water flow occurred from the bottom to the top surface of the tape. As was previously mentioned, the consolidation of the latex particles by coalescence is expected to occur in the later stage of the drying process as the volume fraction of latex particles approaches 0.6. This resulted in the formation of latex particle clusters that migrated in the same direction as the solvent, to the top

surface, as drying proceeded. Therefore, the top surface of the cast tapes could be comprised by an assembly of latex particle clusters, whose interstices provided an open pore structure. A similar behavior was found by Martinez et al. [21] who studied the drying process of aqueous Al_2O_3-latex tape cast layers. They observed the formation of particle clusters in the top surface of the cast tapes as the solids volume fraction increased during drying. The pronounced formation of particle clusters indicated that the latex particles might undergo a consolidation by coalescence at high solid loading which resulted in an increase in the pore size of the green tape. In addition, the latex coalescence increased the pore size left by the latex during burnout. These large pores reduced the YSZ sintering rate within the matrix leading to retained closed porosity in the sintered tapes. Thus, the coalescence of the latex particles affected the green and sintered microstructure of the tapes, conducting to a greater porosity. This porosity was principally found in the top surface due to the migration of the consolidated latex particles during drying.

Conclusions

Porous YSZ tapes with volume fraction of porosity from 28.9 to 53% were developed using starch as a pore-forming agent.

Two kinds of pores were observed in the sintered tapes: large pores created by the starch particles with lengths between 15 and 80 μm and smaller pores in the matrix with lengths between 0.6 and 3.8 μm. The coalescence of the latex particles during the drying of the cast tapes and the pore coalescence during sintering, might contribute to the enlargement of the pores in the matrix, reducing the sinterability of the YSZ and leading to closed porosity in the sintered tapes. Consequently, the porosities were above those predicted for all the starch contents examined.

The larger deviations from the predicted porosity, as more starch was added, were attributed to the reduction in the YSZ packing density within the matrix. The total porosity of the tapes with starch followed that predicted, based on the volume fraction of starch in the green tape and the additional porosity created by the adjustments of the formulation (higher F_{VL}/F_{VZ} ratio with increasing added starch).

Differences between the top and bottom surfaces of the tapes sintered at 1600 °C for all the starch contents used were found, the top surface of the sintered tapes had a greater porosity than the bottom one. The migration of the consolidated latex particles to the top surface during drying produced an increase in both: the pore size of the cast tapes and the pore size left by the latex during burnout, thereby decreasing the YSZ sintering rate within the matrix and leading to a greater porosity of the top surface.

The porosity was completely open for the tapes sintered at 1000 and 1300 °C for the different starch contents. The open pores between the YSZ particles were removed by sintering at 1600 °C. For the tapes with 0 and 17.6 vol.% starch sintered at 1600 °C, there was no open porosity; for starch contents ≥28.4vol.% the open porosity corresponded to the connecting channels between the overlapping starch pores which resulted in a connected porous network in the sintered body. As the volume fraction of starch increased from 17.6 to 37.8 vol.%, there was a gradual increase in the volume and size of the connecting channels between pores, and consequently in the openness of the pore structure. For 37.8 vol.% starch open porosity was predominant in the microstructure.

Acknowledgements The authors would like to acknowledge CONICET (Argentina), NSERC (Canada), and CNPq (Brazil) for provision of research funding through the Inter-American Research in Materials (CIAM) Program. We also acknowledge the support of the Canada Foundation for Innovation, the Atlantic Innovation Fund, and other partners who helped fund the Facilities for Materials Characterization, managed by the Dalhousie University Institute for Materials Research, who provided access to the FE-SEM.

References

1. Ishizaki K, Komarneni S, Nauko M (1998) Porous materials process technology and applications. Kluwer, London
2. Saggio-Woyanski RJ, Scott CE, Minnear WP (1992) Am Ceram Soc Bull 71:1674
3. Rambo CR, Cao J, Seiber H (2004) Mater Chem Phys 87:345
4. Boaro M, Vohs JM, Gorte RJ (2003) J Am Ceram Soc 86(3):395
5. Prathar SK, Dassharma A, Maiti HS (2007) J Mater Sci 42(17): 7220. doi:10.1007/s10853-007-1497-x
6. Jiang SP, Chan SH (2004) J Mater Sci 39(14):4405. doi:10.1023/B:JMSC.0000034135.52164.6b
7. Corbin SF, Apté PS (1999) J Am Ceram Soc 82(7):1693
8. Zivcova Z, Gregorová E, Pabst W (2007) J Mater Sci 42(20): 8760. doi:10.1007/s10853-007-1852-y
9. Gregorová E, Pabst W, Bohačenko I (2006) J Eur Ceram Soc 26:1301
10. Gregorová E, Pabst W (2007) J Eur Ceram Soc 27:669
11. Moreno R (1992) Am Ceram Soc Bull 71(11):1647
12. Moreno R (1992) Am Ceram Soc Bull 71(10):1521
13. Kristofferen A, Roncari E, Galassi C (1998) J Eur Ceram Soc 18:2123
14. Pagnoux C, Chartier T, de Granja MF, Doreau F, Ferreira JM, Baumard JF (1998) J Eur Ceram Soc 18:241
15. Albano MP, Genova LA, Garrido LB, Plucknett K (2008) Ceram Int 34:1983
16. Smay JE, Lewis JA (2001) J Am Ceram Soc 84(11):2495
17. Kolar D (1979) Mater Sci Res 13:335
18. Gregorová E, Zivcova Z, Pabst W (2006) J Mater Sci 41(18): 6119. doi:10.1007/s10853-006-0475-z
19. Díaz A, Hampshire S (2004) J Eur Ceram Soc 24:413
20. Lyckfeldt O, Ferreira JMF (1998) J Eur Ceram Soc 18:131
21. Martinez CJ, Lewis JA (2002) J Am Ceram Soc 85(10):2409